NANO LETTERS

Letter

pubs.acs.org/NanoLett

Three-Dimensional Optical Trapping and Manipulation of Single Silver Nanowires

Zijie Yan,[†] Justin E. Jureller,[†] Julian Sweet,[‡] Mason J. Guffey,[†] Matthew Pelton,[‡] and Norbert F. Scherer*[,†,‡]

[†]The James Franck Institute, The University of Chicago, 929 East 57th Street, Chicago, Illinois 60637, United States

[‡]Center for Nanoscale Materials, Argonne National Laboratory, 9700 South Cass Avenue, Argonne, Illinois 60439, United States

Supporting Information

ABSTRACT: We report the first experimental realization of all-optical trapping and manipulation of plasmonic nanowires in three dimensions. The optical beam used for trapping is the Fourier transform of a linearly polarized Bessel beam (termed FT-Bessel). The extended depth of focus of this beam enables the use of a retroreflection geometry to cancel radiation pressure in the beam propagation direction, making it possible to trap highly scattering and absorbing silver nanowires. Individual silver nanowires with lengths of several micrometers can be positioned by the trapping beam with a precision better than 100 nm and are oriented by the polarization of the trapping light with a precision of approximately 1°. Multiple nanowires can be trapped simultaneously in spatially separated maxima of the trapping field. Since trapping in the interferometric FT-Bessel potential is robust in bulk solution and near surfaces, it will enable the controlled assembly of metal nanowires into plasmonic nanostructures.

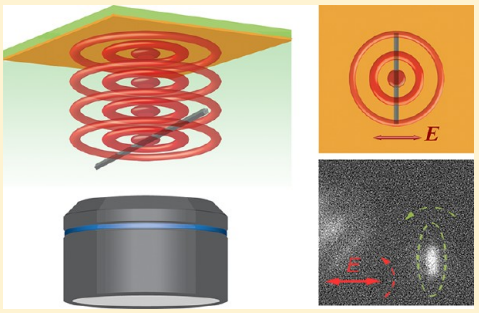

KEYWORDS: *Optical tweezers, optical manipulation, plasmonics, metal nanowires*

Silver (Ag) nanowires have the potential to serve as elements in nanoscale photonic circuits: surface plasmons in these wires are capable of confining light laterally well below the diffraction limit, and the confined fields can propagate over distances of 10 μm or longer.[1−5] In order for Ag nanowires to serve as functional elements in nanophotonic systems, it will be necessary to position and align them in three dimensions with nanometer-scale precision. Several techniques have been developed to align large numbers of nanowires and deposit them on substrates, including fluidic alignment[6] and Langmuir−Blodgett patterning,[7] that offer more control than simple drop or spin-casting.[2,3,8,9] Still, rational and versatile manipulation of individual metal nanowires remains a challenge.[10−13] One can use a mechanical probe to push an Ag nanowire along the substrate, and this method has been used to fabricate hybrid circuits using Ag and ZnO nanowires.[4] However, this mechanical assembly is not suitable for controlling the position and orientation of the nanowires in three dimensions and also risks damaging the material.

Optical forces offer a promising approach to position and orient nanoscale objects. Conventional optical tweezers, consisting of a tightly focused Gaussian beam, have been used to trap semiconductor nanowires,[11,14−16] as well as small metal nanoparticles, including spheres, bipyramids, and nanorods.[17−22] However, as the length of Ag nanorods increases, the resultant multiple longitudinal plasmon modes can couple with the incident laser light, and the radiation pressure due to absorption and scattering of light increases.[1,5,22,23] When the object can be considered a nanowire (an aspect ratio of > 10),[24] radiation pressure in the beam propagation direction dominates over the attractive gradient force, and stable trapping of Ag nanowires in simple Gaussian beams is not possible.[11]

The destabilizing effects of the forward radiation pressure can be overcome by pushing the nanowires against a substrate, so that the movement in the beam propagation direction is hindered.[13,25] Using this method, Tong et al. made the important observation that Ag nanowires tend to align perpendicularly to the polarization of the trapping laser,[13] thus providing a route to control the orientation of an Ag nanowire. However, translation of Ag nanowires was not demonstrated in this work, and it is possible that the Ag nanowires adhered to the substrate via nonspecific interactions.[26,27] Stable trapping and translation of Ag nanowires on a surface was demonstrated using a novel opto-electronic tweezers method,[27] but this does not allow controlled orientation of the nanowires, and manipulation is limited to the two-dimensional surface. We have recently demonstrated stable trapping of Ag nanowires that can be translated and oriented at surfaces using spatially extended optical fields.[25]

In this Letter, we overcome the aforementioned limitations and report the first experimental realization of three-dimensional (3D) optical trapping and control over position and orientation of Ag nanowires in bulk solution.

Received: June 3, 2012

dx.doi.org/10.1021/nl302100n | *Nano Lett.* XXXX, XXX, XXX−XXX

Three-Dimensional Trap Configuration. Two requirements must be satisfied to form stable 3D traps for Ag nanowires. First, the light field must be tightly confined, so that it exerts strong, attractive gradient forces. Second, the radiation pressure in the beam propagation direction needs to be compensated. Both can be accomplished by using two counter-propagating beams brought to a common focus.[28] The potential versatility of such a trap is partially offset by the complexity of aligning the counter-propagating traps, including matching the spatial profiles. Alternatively, the requirements can be achieved by retroreflection of a single beam from a mirror. In this case, the challenge is to locate the focus of the reflected beam in the same axial position as the focus of the incident beam and to have good spatial overlap.[29,30] Zero-order Bessel beams (ZOBBs) make this possible through their extended depth of focus, since they are nearly "diffraction-free" over long distances.[31] At the same time, ZOBBs provide strong localization of the optical field in the transverse direction, enabling the lateral trapping of Ag nanowires.[25] Three-dimensional Bessel-beam traps have been generated both in a counter-propagating beam configuration[32] and using a dielectric mirror[33] and have been used to trap and manipulate polystyrene microparticles.[33]

To achieve stable 3D trapping of Ag nanowires, we developed a new retroreflection configuration, using the spatial Fourier transform of a Bessel beam rather than the Bessel beam itself for optical trapping. The Fourier transformed Bessel beam (FTBB) is an annular ring, but it quickly evolves into another Bessel-like beam along the propagation direction (see Supporting Information, Figure S1). Compared to a conventional ZOBB, the FTBB has a longer propagation length and less variation of the central intensity along the propagation direction; both of these characteristics facilitate the formation of a 3D trap. We refer to the result as an interferometric Fourier transformed Bessel beam (IFTB) trap.

A schematic diagram of the experimental setup is shown in Figure 1a. The experiments were performed with an inverted microscope (Olympus IX71). A linearly polarized beam from a home-built Ti:Sapphire laser (emitting at a wavelength of 800 nm) was shaped into a symmetric Gaussian profile using a spatial filter, and the Gaussian beam was shaped into the desired FT-Bessel beam using a spatial light modulator (SLM; Hamamatsu Photonics, X10468).[34] The SLM modifies the incident field as:

$$E(r) = A(r)e^{i2\pi r/a}e^{i2\pi r^2 b} \quad (1)$$

where r denotes the radial coordinate and $A(r)$ is the amplitude of the incident Gaussian beam. The first exponential term represents the axicon phase function that generates a Bessel beam,[35] and the second term signifies a Fresnel lens that shifts the beam focus along the propagation direction.[36] The parameter a is adjusted to control the diameter and depth of focus of the Bessel beam.[31] The shaped beam was relayed by two lenses and a dichroic mirror to the back aperture of a 40X microscope objective (NA 0.9, Olympus UPLSAPO), which performed a spatial Fourier transform of the incident field. A half-waveplate located after the dichroic mirror was used to control the polarization of the trapping field. The FT-Bessel beam was shifted along the propagation direction (denoted as the z-direction) by adjusting the parameter b in eq 1, so that the maximum intensity of the trapping field was located at the image plane of the objective. The parameters a and b were optimized empirically to the values $a = 5 \times 10^{-4}$ m and $b = -4.50 \times 10^{6}$ m^{-2}. The laser power after the objective was measured to be approximately 100 mW.

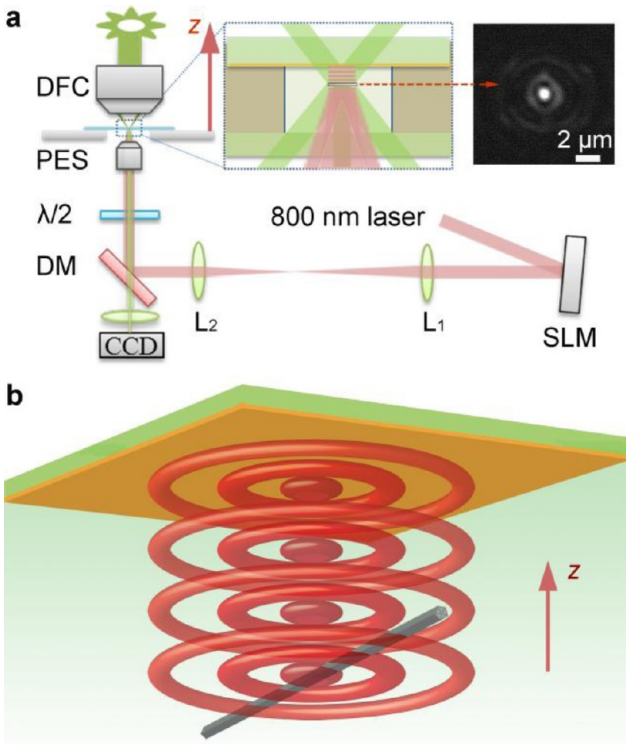

Figure 1. (a) Schematic of the experimental setup used for three-dimensional manipulation of Ag nanowires. DFC: dark-field condenser; PES: piezoelectric stage; $\lambda/2$: half-waveplate; DM: dichroic mirror; SLM: spatial light modulator. The focal lengths of the lenses L_1 and L_2 are 75 and 50 cm, respectively. The incident beam propagates in the z-direction. The Bessel beam generated at the image plane (defined as $z = 0$, which is also the trapping plane) is shown on the right. The sample cell consists of a dichroic mirror on the top and a coverslip at the bottom. (b) Illustration of the interferometric Fourier-transform Bessel beam (IFTB) trap.

In the retroreflection configuration, the reflected beam interferes with the incident beam, resulting in periodic bright and dark planes (i.e., planes of constructive and destructive interference) along the propagation direction.[32,33] The IFTB trap can thus be thought of as a 3D optical lattice, as illustrated in Figure 1b. In each of the interference planes, the beam consists of a central spot surrounded by several concentric rings, as shown in the inset of Figure 1a.

Trapping of Single Silver Nanowires. Silver nanowires were synthesized via a polyol method.[37] The nanowires produced had lengths ranging from approximately 1 to 20 μm and diameters ranging from approximately 50 to 150 nm (see Supporting Information, Figure S2). The sample cell, containing a droplet of the nanowire aqueous solution, was built by placing a 130-μm thick silicone spacer between a coverslip at the bottom and a custom dichroic mirror (Precision Photonics) at the top (see Supporting Information for alternative choices of the mirror). The mirror reflects the laser beam and transmits visible light, allowing the trapped nanowires to be imaged using dark-field microscopy. The position of the optical trap, and thus of the trapped nanowires, was fixed, and translation of the trapped nanowires was

dx.doi.org/10.1021/nl302100n | Nano Lett. XXXX, XXX, XXX−XXX

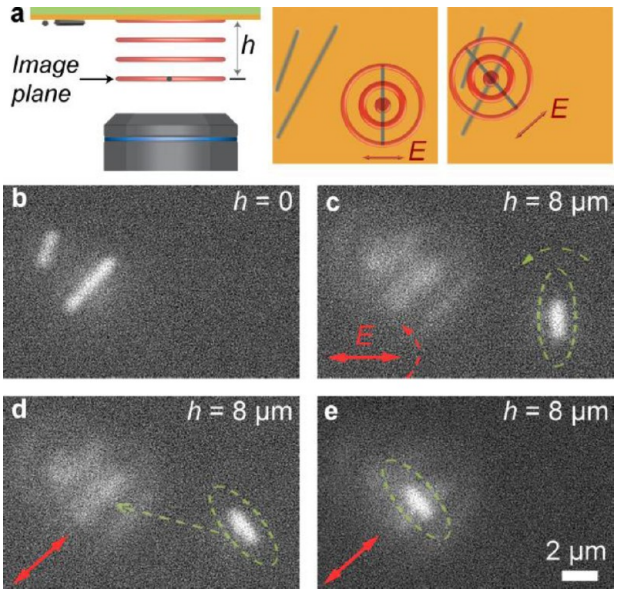

Figure 2. (a) Illustration of three-dimensional optical trapping and manipulation of Ag nanowires. The distance from the image plane to the mirror surface is defined as h. The position of a trapped nanowire can be determined relative to stationary Ag nanowires that are stuck on the mirror surface. The orientation of the nanowire in solution is controlled by the beam polarization. (b) Dark-field image of two stationary Ag nanowires on the mirror surface. After this image was taken, the surface was moved 8 μm away from the image plane. The out-of-focus image of the stationary nanowires subsequently serves as a reference. (c) A trapped and aligned Ag nanowire with the mirror in this new position. (d) Rotation of the nanowire with the polarization of the trapping beam. (e) Translation of the nanowire with the position of the trapping beam.

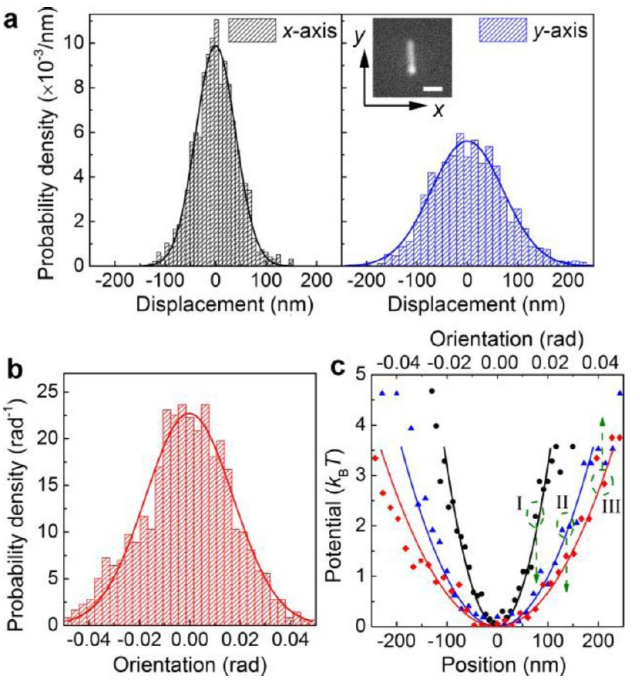

Figure 3. Probability densities of (a) the displacement along the x-axis and the y-axis, and (b) the orientation of an Ag nanowire trapped by the central spot at $h = 6$ μm. Also shown are normalized Gaussian fits: $P(\xi) = (2\pi\sigma^2)^{-1/2}\cdot\exp\{-0.5[(\xi - \mu)/\sigma]^2\}$, where σ and μ are fitting parameters and ξ is x, y, or θ. An image of the nanowire is shown in the inset of the second panel. The scale bar is 2 μm. (c) The corresponding potentials of mean force of the central trapping spot: (I) x-axis, (II) y-axis, and (III) orientation. The fitted curves are quadratic functions: $U(\xi) = 0.5[(\xi - \mu)/\sigma]^2$, where σ and μ are from the corresponding fits of the probability densities to the normal distribution. Values of the fitting parameters are given in Table 1.

achieved by moving the sample cell in three dimensions using a piezoelectric stage (Physik Instrumente, E-710).

Figure 2 demonstrates the 3D trapping of an Ag nanowire. Stationary nanowires fixed on the mirror surface serve as a spatial reference. The orientation of the trapped Ag nanowire was always perpendicular to the polarization of incident light,[25] so we could readily orient the nanowire in any direction by rotating the half-waveplate (Figure 2d). As shown in Figure 2e, the nanowire could also be translated to any position in the image plane and nanowires could also be trapped at different distances from the mirror surface. The trap was robust, as demonstrated by the fact that the nanowire remained stable even when the central spot had been positioned above another nanowire that was stuck to the surface. Scattering from the stationary nanowire, and from the trapped nanowire itself, does not significantly degrade the quality of the trap, due to the "self-healing" nature of the Bessel beam.[38]

The trapped Ag nanowires were generally 1−6 μm in length, since longer nanowires usually settled to the bottom of the sample cell before being trapped. This sedimentation could be ameliorated by adjusting the buoyancy. We note that the IFTB optical tweezers could also easily trap small particles that were present in the solution as a byproduct of the nanowire synthesis (see Supporting Information, Figure S2c).

Trapping Potential and Stiffness. The inset in the second panel of Figure 3a shows an Ag nanowire with a length of approximately 3.5 μm trapped in the central spot of the Bessel beam. Figure 3a shows the distribution of positions of the centroid of the nanowire in the trap; larger fluctuations are observed along the long axis of the wire (denoted as the y-direction) than along the short axis (denoted as the x-direction). Figure 3b shows the distribution of nanowire orientational angles, θ; the standard deviation of orientation was found to be only 1°.

Table 1. Fitting Parameters in Figure 3

ξ	σ	μ
x-axis	39.6 nm	−0.1 nm
y-axis	71.3 nm	−0.5 nm
orientation	0.017 rad	0

Using the distributions of position and orientation, we can estimate the corresponding trapping potentials. The potential of mean force, pmf(ξ), is determined from the measured probability density functions:

$$\mathrm{pmf}(\xi) = -k_B T \ln P(\xi) \quad (2)$$

where k_B is Boltzmann's constant, T is absolute temperature, and $P(\xi)$ is the probability density of the parameter ξ (x, y, or θ). Figure 3c shows the calculated trapping potentials, where pmf(0) is set to be zero. The potential depth is 2.2 k_BT and 1.0 k_BT for a displacement of 100 nm in the x- and y-directions, respectively, and it is 1.2 k_BT for a rotation of 1.5°. These values are larger than that of thermal fluctuations (0.5 k_BT for each degree of freedom), so that this nanowire, which is a representative example, is stably trapped. We experimentally measured stable trapping of many other individual nanowires,

dx.doi.org/10.1021/nl302100n | Nano Lett. XXXX, XXX, XXX−XXX

as well, and observed trapping times in excess of 15 min. The most common reason that a trapped nanowire would leave is because of perturbation from another nanowire entering the trap rather than spontaneously due to thermal fluctuations.

Assuming the minimum of the trapping potential is harmonic, the positional stiffness of the trap, κ, can be evaluated from the variance of the nanowire position through the equipartition theorem:[39]

$$\frac{1}{2}k_B T = \frac{1}{2}\kappa\langle\xi^2\rangle \quad (3)$$

Figure 4a,b summarizes the measured positional and angular stiffness of the central spot as a function of the nanowire length, L. For the estimation of angular stiffness, we use the small-angle approximation, $\sin(\theta) \approx \theta$. Nanowires were trapped at different distances from the mirror surface, but we found that the stiffness of the trap is insensitive to the distance (see Supporting Information, Figure S4). As shown in Figure 4a, the positional stiffness along both the short and long axes are on the order of 1 pN/μm, with the stiffness being greater along the short axis. Generally, the trap stiffness decreases when the length of the nanowire increases. A similar trend exists for the angular stiffness as shown in Figure 4b, with a typical angular stiffness on the order of 10^{-17} J/rad^2. For reference, we also estimated the trapping efficiency of the central spot by trapping latex beads with a diameter of 500 nm. In this case, the stiffness of the IFTB trap is 4.2 ± 0.4 pN/μm at h = 4 μm and 3.5 ± 0.4 pN/μm at h = 8 μm.

Trapping Efficiency. An alternative method of evaluating the trapping force is to move the sample cell at a constant speed and measure the escape velocity, ν_{esc}, at which the nanowire leaves the trap. The moving fluid exterts a viscous drag force on the nanowire, described by Stokes' law: $F_d = c_d\nu_{esc}$, where c_d is the drag coefficient.[26] For a prolate spheroid with aspect ratio $\alpha \gg 1$ moving perpendicular to its long axis, c_d is given by[40]

$$c_d = \frac{4\pi\eta L}{\ln(2\alpha) + 0.5} \quad (4)$$

where η is the dynamic viscosity of the fluid (in this case, water) and L is the length of the spheroid. The lengths of the trapped nanowires were determined from the dark-field images; the much smaller diameters were estimated as the mean diameter of the wires in the sample (d = 88 nm) as measured by scanning electron microscopy. Since the energy of a Bessel beam is approximately equally distributed between the central spot and the surrounding rings,[35] we estimated the power of the central spot to be 33 mW and used this to calculate a (conservative) trapping efficiency, i.e., the trapping force normalized to the trapping laser power. As shown in Figure 4c, the trapping efficiency is essentially constant at a value near 0.05 pN/mW, independent of nanowire length. For a reference sample of 500 nm dia. latex beads, we measured a similar trapping efficiency of approximately 0.08 pN/mW.

A previous study on optical trapping of single gold nanorods with diameters of 20−50 nm and lengths of 50−90 nm measured transverse trapping constants around 0.01 pN/(nm·W).[21] In our experiments, the typical stiffness of 1 pN/μm of the central spot corresponds to a trapping constant of 0.03 pN/(nm·W). It seems surprising that the trap stiffness for Ag nanowires in the IFTB trap is even larger than the stiffness for Au nanorods in a Gaussian-beam trap, especially since the central spot of the IFTB trap is rather large: one might expect

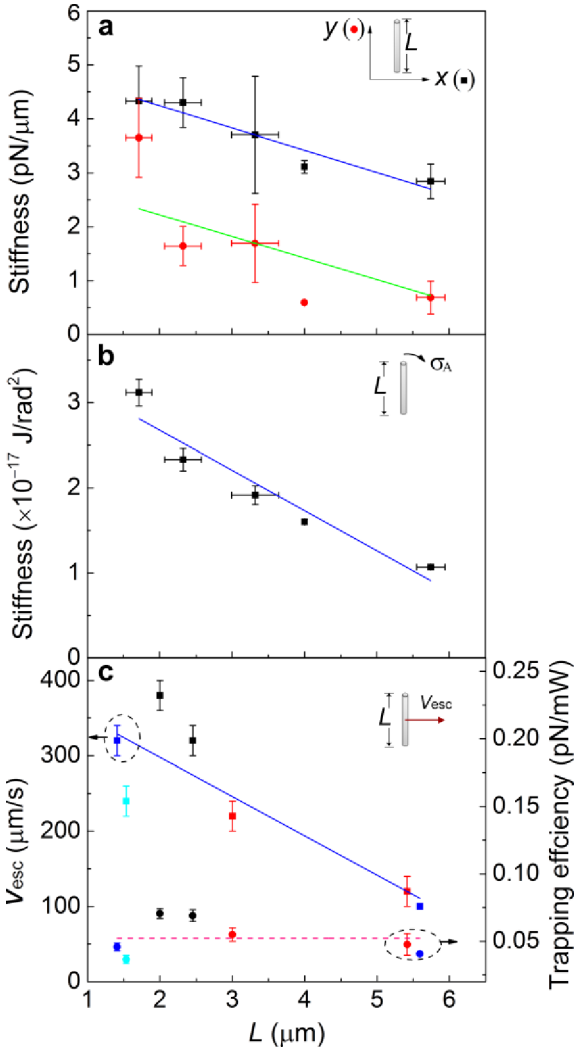

Figure 4. (a) Stiffness of trapping in the x- and y-directions for a single Ag nanowire in the central spot of the Bessel beam. (b) Stiffness of nanowire orientation in the central spot of the Bessel beam. For a and b, the data points are mean values for 23 individual Ag nanowires, categorized by wire length with bin size of 1 μm and weighted according to the corresponding trajectory times (see Supporting Information, Figure S4). The vertical error bars reflect the standard deviation of the weighted average in each bin, and the horizontal error bars reflect the standard deviation of L. Note that only one nanowire contributes to the bin of 4−5 μm. (c) The results of constant-velocity Stokes drag measurements. The escape velocity (ν_{esc}) of a single Ag nanowire and the corresponding trapping efficiency of the central spot are shown in the plot. Color indicates the distance from the image plane to the mirror surface: black h = 2 μm; cyan h = 4 μm; blue h = 8 μm; red h = 12 μm. Lines are linear fits of the data.

that the transverse gradient force would be much smaller than that obtained for tightly focused Gaussian beams. However, we believe that the cancellation of the axial (z-direction) radiation pressure (scattering force) allows only a pure gradient force to remain as opposed to a net gradient force in the non-interferometric Gaussian beam trap. In addition, the extended length of the Ag nanowires can produce stronger overall interactions with the trapping laser.

The strong orientational trapping is consistent with previous reports that the orientation of plasmonic nanoparticles is controlled by the light polarization.[13,25] We showed previously that the torque resulting from the dot-product of the

dx.doi.org/10.1021/nl302100n | Nano Lett. XXXX, XXX, XXX−XXX

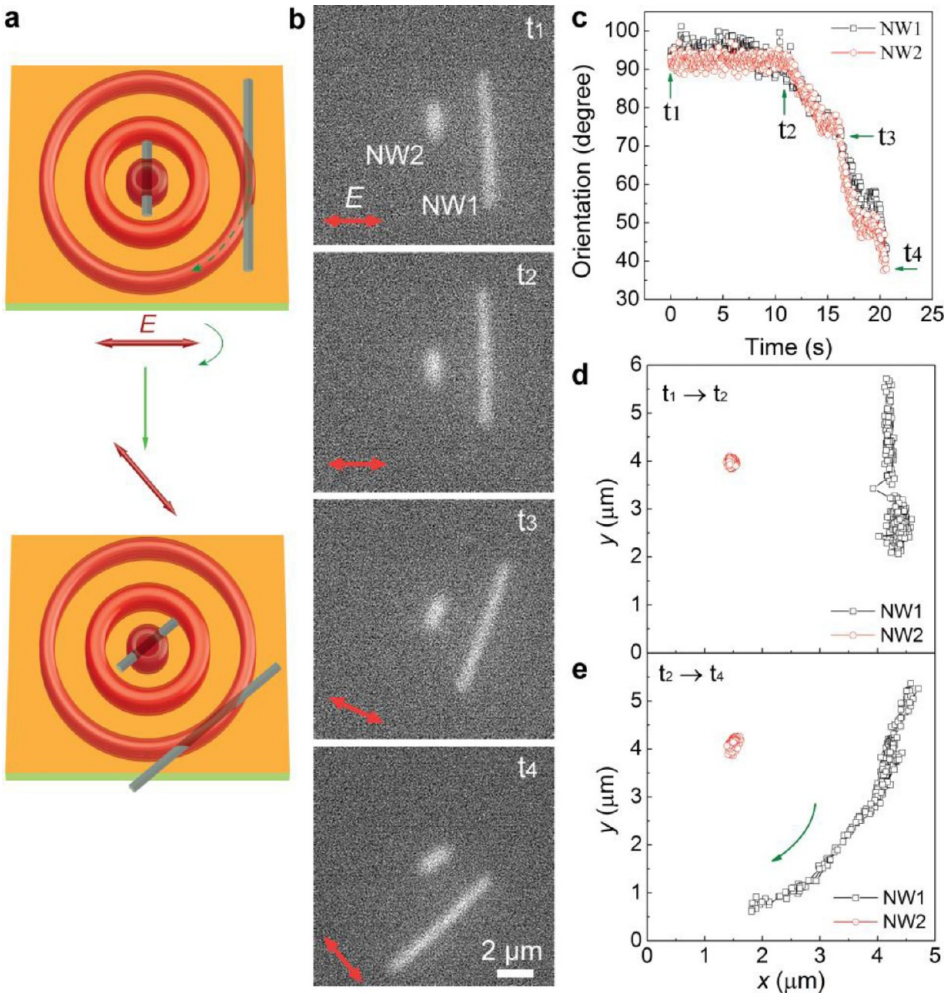

Figure 5. (a) Illustration of simultaneous trapping of Ag nanowires by the central spot and a side ring of the Bessel-beam trap. As the trapping-laser polarization is rotated, the nanowire trapped on the side moves along the ring, maintaining a tangential orientation. (b) Experimental demonstration of simultaneous trapping and rotation of two Ag nanowires at $h = 4$ μm (see Supporting Information, Movie S2). The first nanowire (NW1) was trapped by a ring, and the second (NW2) was trapped by the central spot. The beam polarization was fixed from time t_1 to t_2 and rotated continually from t_2 to t_4. (c) Trajectories of orientation and (d, e) trajectories of centroid positions of the two nanowires. The time interval between data points is 1/30 s.

transmission dipole of a nanoparticle (i.e., Au nanorods[41] and bipyramids[18,19]) with a linearly polarized trapping beam prevented free rotational motion of the nanoparticle. Recently, in experiments and finite-difference time-domain simulations of Ag nanowires trapped in two dimensions at a transparent dielectric surface, we found that the field-induced torque is large compared with thermal energy, so that Ag nanowires could be oriented in a variety of linearly polarized optical field patterns.[25]

Trapping of Multiple Nanowires. The rings of the interfering FT-Bessel beam can also trap Ag nanowires in 3D space, independent of trapping in the central spot. Nanowires trapped in the rings are always oriented with their long axis tangential to the rings and perpendicular to the light polarization. Rotating the polarization therefore moves the nanowire along the rings, as illustrated in Figure 5a and demonstrated in Figures 5b–e. Trapping by a ring is generally less stable than that by the central spot, as indicated by Figure 5d: the position of a nanowire trapped in a ring fluctuated over several micrometers along the long axis, even when the beam polarization was fixed, while a nanowire trapped in the central spot maintained a much more steady position. After approximately 20 s, the nanowire trapped in the ring escaped, while the one in the central spot remained trapped.

We also observed simultaneous trapping of Ag nanowires in multiple planes along the beam propagation direction, as shown in Figure 6a. By changing the position of the mirror relative to the focus and thus the locations of the standing-wave maxima, it was possible to move the nanowire from one intensity maximum to another. The IFTB optical tweezers could also trap a single Ag nanowire using the maximum in several planes, so that it is oriented vertically with its long axis pointing along the beam propagation direction. This is illustrated in Figure 6c, and demonstrated experimentally in Figure 6b for a nanowire in the central spot and in Figure 6d for a nanowire in a ring. The orientation of the nanowire can be changed by the viscous force induced by moving the sample cell (see Figure 6b), or by the perturbation induced by changing the polarization of the light, as demonstrated in Figure 6e. Figure 6e also shows that two nanowires that have been trapped and oriented can be translated onto two stationary nanowires on the mirror surface, resulting in a complex 3D configuration of multiple nanowires with two nanowires on the surface and the other two in the solution. The versatility and control provided by the IFTB trap

dx.doi.org/10.1021/nl302100n | Nano Lett. XXXX, XXX, XXX–XXX

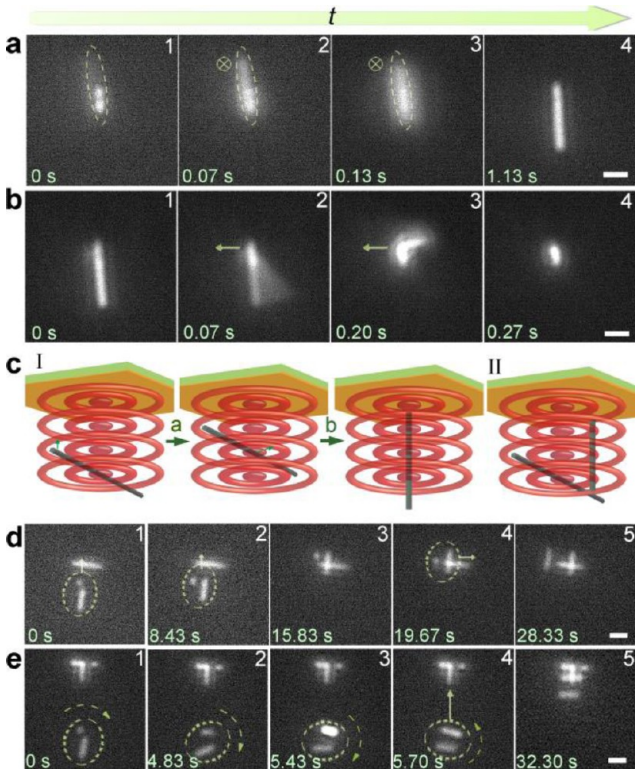

Figure 6. (a) Demonstration of simultaneous trapping of two Ag nanowires in different planes. Initially, a shorter nanowire was trapped in the image plane at h = 8 μm, and a second, longer wire was located out of the image plane, indicated by the dotted ellipse in panel 1. Starting from panel 2, h was increased to 18 μm within 0.1 s, kept fixed for 1 s, and then returned to 8 μm. As a result, the longer Ag nanowire was trapped in the image plane (panel 4). (b) Demonstration of alignment of a trapped nanowire along the beam propagation direction. Panel 1 shows a trapped nanowire originally oriented in the image plane. Starting from panel 2, the nanowire was moved to the left at a velocity of 100 μm/s. Panel 4 shows that this resulted in the nanowire being reoriented vertically. (c) I. Illustration of the manipulations shown in a and b. II. Illustration of two nanowires trapped in different orientations, as in d. (d) Simultaneous manipulation of two nanowires trapped at h = 2 μm. The first nanowire was oriented in the image plane, and the second was oriented along the beam propagation direction. Both nanowires were moved relative to a fixed nanowire on the mirror surface. (e) Changing the orientation of a nanowire, trapped by a ring of the Bessel beam, from the beam propagation direction to the image plane by rotating the polarization direction. The reoriented nanowire and a second trapped nanowire were then moved relative to a pair of fixed nanowires on the mirror surface. The white scale bars are 2 μm. See Supporting Information, Movie S3 for a and b, and Movie S4 for d and e.

make it possible to manipulate and assemble Ag nanowires in 3D space.

In summary, we have demonstrated that Ag nanowires can be trapped, translated, and oriented arbitrarily in three dimensions using structured optical fields; specifically, our optical trap is formed by interfering a linearly polarized, Fourier-transformed zero-order Bessel beam with its own reflection. The robustness of the Bessel beam trap makes it useful for constructing complex 3D assemblies of Ag nanowires or other nanostructures. We envision the interferometric Fourier-transform Bessel trap as a tool for the assembly of 3D plasmonic nanocircuits. For this purpose, the surface properties of both the nanowires and the mirror surface have to be controlled, so that interactions between nanowires and the substrate surface are weak or repulsive;[42] in addition, it will be necessary to immobilize the trapped nanowires once they are moved into place, potentially using photopolymerizable materials.[27] We expect that the trap could be also used to trap and manipulate nanowires made of Au or other metals (in fact we have already obtained confirming preliminary results for Au nanowires), semiconductor nanowires, and other highly scattering or absorbing nanostructures; this would allow for the fabrication of active, 3D hybrid nanophotonic circuits.

■ ASSOCIATED CONTENT

Ⓢ Supporting Information

Movie clips showing the optical manipulation processes; other choices of sample cell preparation; calculation of trapping force from the escape velocity of a latex bead, and additional figures. This material is available free of charge via the Internet at http://pubs.acs.org.

■ AUTHOR INFORMATION

Corresponding Author

*E-mail: nfschere@uchicago.edu.

Notes

The authors declare no competing financial interest.

■ ACKNOWLEDGMENTS

We acknowledge support from the U.S. Department of Energy (DOE), Office of Science, Division of Chemical, Geological and Biological Sciences under Contract No. DE-AC02-06CH11357. This work was also supported in part by the National Science Foundation (CHE-0802913). We thank Dr. Qiti Guo for assistance with the use of central facilities of the NSF-Materials Research Science (MRSEC; DMR-0820054). Use of the Center for Nanoscale Materials was supported by the U. S. Department of Energy, Office of Science, Office of Basic Energy Sciences, under Contract No. DE-AC02-06CH11357.

■ REFERENCES

(1) Ditlbacher, H.; Hohenau, A.; Wagner, D.; Kreibig, U.; Rogers, M.; Hofer, F.; Aussenegg, F. R.; Krenn, J. R. *Phys. Rev. Lett.* **2005**, *95*, 257403.

(2) Sanders, A. W.; Routenberg, D. A.; Wiley, B. J.; Xia, Y.; Dufresne, E. R.; Reed, M. A. *Nano Lett.* **2006**, *6*, 1822−1826.

(3) Knight, M. W.; Grady, N. K.; Bardhan, R.; Hao, F.; Nordlander, P.; Halas, N. J. *Nano Lett.* **2007**, *7*, 2346−2350.

(4) Guo, X.; Qiu, M.; Bao, J.; Wiley, B. J.; Yang, Q.; Zhang, X.; Ma, Y.; Yu, H.; Tong, L. *Nano Lett.* **2009**, *9*, 4515−4519.

(5) Wild, B.; Cao, L.; Sun, Y.; Khanal, B. P.; Zubarev, E. R.; Gray, S. K.; Scherer, N. F.; Pelton, M. *ACS Nano* **2012**, *6*, 472−482.

(6) Huang, Y.; Duan, X. F.; Wei, Q. Q.; Lieber, C. M. *Science* **2001**, *291*, 630−633.

(7) Tao, A.; Kim, F.; Hess, C.; Goldberger, J.; He, R.; Sun, Y.; Xia, Y.; Yang, P. *Nano Lett.* **2003**, *3*, 1229−1233.

(8) Garnett, E. C.; Cai, W.; Cha, J. J.; Mahmood, F.; Connor, S. T.; Christoforo, M. G.; Cui, Y.; McGehee, M. D.; Brongersma, M. L. *Nat. Mater.* **2012**, *11*, 241−249.

(9) Solis, D.; Chang, W.-S.; Khanal, B. P.; Bao, K.; Nordlander, P.; Zubarev, E. R.; Link, S. *Nano Lett.* **2010**, *10*, 3482−3485.

(10) Yan, R.; Pausauskie, P.; Huang, J.; Yang, P. *Proc. Natl. Acad. Sci. U.S.A.* **2009**, *106*, 21045−21050.

(11) Pauzauskie, P. J.; Radenovic, A.; Trepagnier, E.; Shroff, H.; Yang, P. D.; Liphardt, J. *Nat. Mater.* **2006**, *5*, 97−101.

(12) Yan, R.; Gargas, D.; Yang, P. *Nat. Photon.* **2009**, *3*, 569−576.

(13) Tong, L.; Miljkovic, V. D.; Käll, M. *Nano Lett.* **2010**, *10*, 268−273.
(14) Agarwal, R.; Ladavac, K.; Roichman, Y.; Yu, G. H.; Lieber, C. M.; Grier, D. G. *Opt. Express* **2005**, *13*, 8906−8912.
(15) Irrera, A.; Artoni, P.; Saija, R.; Gucciardi, P. G.; Iati, M. A.; Borghese, F.; Denti, P.; Iacona, F.; Priolo, F.; Marago, O. M. *Nano Lett.* **2011**, *11*, 4879−4884.
(16) Wang, F.; Reece, P. J.; Paiman, S.; Gao, Q.; Tan, H. H.; Jagadish, C. *Nano Lett.* **2011**, *11*, 4149−4153.
(17) Svoboda, K.; Block, S. M. *Opt. Lett.* **1994**, *19*, 930−932.
(18) Toussaint, K. C., Jr.; Liu, M.; Pelton, M.; Pesic, J.; Guffey, M. J.; Guyot-Sionnest, P.; Scherer, N. F. *Opt. Express* **2007**, *15*, 12017−12029.
(19) Pelton, M.; Liu, M. Z.; Kim, H. Y.; Smith, G.; Guyot-Sionnest, P.; Scherer, N. E. *Opt. Lett.* **2006**, *31*, 2075−2077.
(20) Bosanac, L.; Aabo, T.; Bendix, P. M.; Oddershede, L. B. *Nano Lett.* **2008**, *8*, 1486−1491.
(21) Selhuber-Unkel, C.; Zins, I.; Schubert, O.; Sönnichsen, C.; Oddershede, L. B. *Nano Lett.* **2008**, *8*, 2998−3003.
(22) Hansen, P. M.; Bhatia, V. K.; Harrit, N.; Oddershede, L. *Nano Lett.* **2005**, *5*, 1937−1942.
(23) Link, S.; El-Sayed, M. A. *J. Phys. Chem. B* **1999**, *103*, 8410−8426.
(24) Chen, J.; Wiley, B. J.; Xia, Y. *Langmuir* **2007**, *23*, 4120−4129.
(25) Yan, Z. J.; Sweet, J.; Jureller, J. E.; Guffey, M. J.; Pelton, M.; Scherer, N. F. *ACS Nano* **2012**, DOI: 10.1021/nn302795j.
(26) Grigorenko, A. N.; Roberts, N. W.; Dickinson, M. R.; Zhang, Y. *Nat. Photon.* **2008**, *2*, 365−370.
(27) Jamshidi, A.; Pauzauskie, P. J.; Schuck, P. J.; Ohta, A. T.; Chiou, P.-Y.; Chou, J.; Yang, P.; Wu, M. C. *Nat. Photon.* **2008**, *2*, 85−89.
(28) Ashkin, A. *Phys. Rev. Lett.* **1970**, *24*, 156−159.
(29) Zwick, S.; Haist, T.; Miyamoto, Y.; He, L.; Warber, M.; Hermerschmidt, A.; Osten, W. *J. Opt. A: Pure Appl. Opt.* **2009**, 11.
(30) Pitzek, M.; Steiger, R.; Thalhammer, G.; Bernet, S.; Ritsch-Marte, M. *Opt. Express* **2009**, *17*, 19414−19423.
(31) Arlt, J.; Garces-Chavez, V.; Sibbett, W.; Dholakia, K. *Opt. Commun.* **2001**, *197*, 239−245.
(32) Čižmar, T.; Šiler, M.; Zemánek, P. *Appl. Phys. B: Laser Opt.* **2006**, *84*, 197−203.
(33) Čižmar, T.; Garces-Chavez, V.; Dholakia, K.; Zemánek, P. *Proc. SPIE* **2004**, *5514*, 643.
(34) Grier, D. G. *Nature* **2003**, *424*, 810−816.
(35) Mazilu, M.; Stevenson, D. J.; Gunn-Moore, F.; Dholakia, K. *Laser Photon. Rev.* **2010**, *4*, 529−547.
(36) Curtis, J. E.; Koss, B. A.; Grier, D. G. *Opt. Commun.* **2002**, *207*, 169−175.
(37) Korte, K. E.; Skrabalak, S. E.; Xia, Y. *J. Mater. Chem.* **2008**, *18*, 437−441.
(38) Garces-Chavez, V.; McGloin, D.; Melville, H.; Sibbett, W.; Dholakia, K. *Nature* **2002**, *419*, 145−147.
(39) Phillips, D. B.; Carberry, D. M.; Simpson, S. H.; Schäfer, H.; Steinhart, M.; Bowman, R.; Gibson, G. M.; Padgett, M. J.; Hanna, S.; Miles, M. J. *J. Opt.* **2011**, *13*, 044023.
(40) Edwards, B.; Mayer, T. S.; Bhiladvala, R. B. *Nano Lett.* **2006**, *6*, 626−632.
(41) Guffey, M. J.; Miller, R. L.; Gray, S. K.; Scherer, N. F. *Nano Lett.* **2011**, *11*, 4058−4066.
(42) Guffey, M. J.; Scherer, N. F. *Nano Lett.* **2010**, *10*, 4302−4308.